

Hyperfine-state-dependent lifetimes along the Ni-like isoelectronic sequence

M. Andersson, K. Yao, R. Hutton, Y. Zou, and C. Y. Chen*

The Key Laboratory of Applied Ion Beam Physics, Ministry of Education, People's Republic of China and Shanghai EBIT Laboratory, Institute of Modern Physics, Fudan University, Shanghai, People's Republic of China

T. Brage

Department of Physics, Lund University, Box 118, SE-221 00 Lund, Sweden

(Received 15 January 2008; published 29 April 2008)

An investigation of the lifetime of the $3d^9 4s\ ^3D_3$ level along a part of the nickel-like isoelectronic sequence has been performed. The focus of this work has been to evaluate the importance of the hyperfine induced electric quadrupole channel of the $3d^{10}\ ^1S_0 - 3d^9 4s\ ^3D_3$ transition for isotopes with nuclear spin. Comparisons between the magnetic octupole transition rate and the hyperfine-induced electric quadrupole transition rate shows that the hyperfine quenching is of importance along the whole isoelectronic sequence. At the low- Z end the hyperfine induced electric quadrupole transition channel dominates, being several orders of magnitude larger than the rate for the magnetic octupole transition channel, while for higher Z the two rates are of comparable size.

DOI: [10.1103/PhysRevA.77.042509](https://doi.org/10.1103/PhysRevA.77.042509)

PACS number(s): 31.30.Gs, 31.10.+z, 32.70.Cs

I. INTRODUCTION

Forbidden transitions play an important role in many branches of physics and they are in general delicate probes of the structure of atomic ions. At the same time they are important tools for diagnostics and modeling of astrophysical and laboratory plasmas. In this paper we will focus on two different kinds of forbidden transitions. The first is a magnetic octupole transition ($M3$), usually modeled as a higher-order correction to the “allowed” electric dipole transitions. The second is a hyperfine induced electric quadrupole (hpf- $E2$), which is opened up in ions with a nonzero nuclear magnetic moment. The interaction between the magnetic moment of the nucleus and the magnetic field created by the electrons will not preserve the total electronic angular momentum, giving rise to mixing between electronic states with different J quantum numbers.

In Ni-like ions the ground term and first excited terms are, for all ions except neutral nickel, $3d^{10}\ ^1S$, $3d^9 4s\ ^3D$, and 1D . The lowest excited level is therefore $3d^9 4s\ ^3D_3$, which can only decay to the ground level 1S_0 through an $M3$ transition, in the absence of nuclear spin. The second excited level, 3D_2 , however has an open $E2$ decay channel to the ground level. Cases such as these, when a level with a dominant magnetic decay of order k is adjacent to a level with a dominant electric decay of order $k-1$, are candidates for important hyperfine quenching.

A somewhat similar well-known example of hyperfine quenching can be found in many two electron systems where the lowest excited term is of the type $nsnp\ ^3P$. In such systems, the $J=0$ level can only decay to the $ns^2\ ^1S_0$ ground level through a two-photon decay, while the neighboring $J=1$ level has a (spin-forbidden) electric dipole ($E1$) decay channel. In the presence of a nuclear spin, the hyperfine induced decay rate from $J=0$ could be important [1,2].

Nickel-like ions have been investigated extensively. On the theoretical side, Dong *et al.* [3] used the MCDF method, while Safronova *et al.* [4] used relativistic many-body perturbation theory. On the experimental side these ions have been studied with beam-foil techniques [5], tokamaks [6], in laser-produced plasmas [7–10] and capillary discharges [11,12]. However, very few of these studies have dealt with the more “exotic” $M3$ decay. The decay of this level was first reported in the x-ray region of the spectra of the highly charged ions Th^{62+} and U^{64+} by Beiersdorfer *et al.* [13] at Lawrence Livermore National Laboratory electron beam ion trap (EBIT). These experimental results were later followed by a theoretical investigation by Biémont *et al.* [14]. Träbert *et al.* [15] did a more detailed investigation of the long-lived 3D_3 in nickel-like xenon, reporting a lifetime of (11.5 ± 0.5) ms. This was about 20–60 % shorter than the theoretical result reported in the same publication, using an average level (AL) multiconfiguration Dirac-Fock (MCDF) method and the earlier result by Safronova *et al.* [16] using relativistic many-body perturbation theory (RMBPT). In Yao *et al.* 2006 [17,18], we showed that the reason for the deviation between experiment and earlier theory is a hpf- $E2$ decay channel, induced by hyperfine interaction between the 3D_3 and 3D_2 levels of the $3d^9 4s$ configuration. In a recent paper by Träbert *et al.* [19] our theoretical results were confirmed by experimental lifetime measurements of pure ^{132}Xe , which has no nuclear magnetic moment, i.e., decay only through an $M3$ transition channel, and ^{129}Xe , with nuclear spin $1/2$ and where the hyperfine level $F=7/2$ decay through only an $M3$ transition channel and $F=5/2$ decays through both an $M3$ and an hyperfine induced $E2$ transition channel.

This paper is an extension of our recent report (Yao *et al.* 2006 [17,18]) and we investigate the lifetime of the $3d^9 4s\ ^3D_3$ level in the Ni-like isoelectronic sequence. From our theoretical investigation of Cu^+ , Mo^{14+} , Pd^{18+} , In^{21+} , Sb^{23+} , I^{25+} , Xe^{26+} , Cs^{27+} , Ba^{28+} , Pr^{31+} , and Nd^{32+} we show that the hyperfine induced $E2$ transition channel is of importance for all isotopes with an nonzero nuclear spin along the

*chychen@fudan.edu.cn

part of the sequence investigated here, i.e., from Cu⁺ ($Z=29$) to Nd³²⁺ ($Z=60$).

II. THEORY

A. Hyperfine interaction

The basic ideas behind hyperfine quenching is that in the presence of a nuclear spin I , an additional hyperfine operator H_{hpf} is introduced into the otherwise electronic Hamiltonian. This Hamiltonian commutes with the total angular momentum $F=J+I$, instead of the total electronic angular momentum J . This hyperfine interaction therefore not only splits the fine structure levels into hyperfine structure levels, but also introduces a wave function mixing between states of different J quantum number and can open new decay channels for some transitions.

The possibility of hyperfine induced transitions was first suggested by Bowen (stated in Ref. [20]). The effect was used as a diagnostic of isotopic composition and densities of low-density plasmas by Brage *et al.* [1]. F -dependent lifetimes due to hyperfine mixing have been measured, in the case of singlet and triplet mixing between $5s19d\ ^1D_2$ and $5s19d\ ^3D_3$ in neutral strontium by Bergström *et al.* [21], and in the $5p^45d\ ^4D_{7/2}$ state of Xe⁺ by Mannervik *et al.* [22].

The hyperfine interaction operator can be described as a multipole expansion (Lindgren and Rosén [23])

$$\mathcal{H}_{\text{hpf}} = \sum_{k \geq 1} \mathbf{T}^{(k)} \cdot \mathbf{M}^{(k)}, \quad (1)$$

where $\mathbf{T}^{(k)}$ and $\mathbf{M}^{(k)}$ are spherical tensor operators of rank k , operating on the electronic and nuclear part of the wave function respectively. We only take the magnetic dipole interaction into consideration and the hyperfine interaction matrix elements can then be expressed as

$$\begin{aligned} \langle \gamma J I F M_F | \mathbf{T}^{(1)} \cdot \mathbf{M}^{(1)} | \gamma' J' I F M_F \rangle &= (-1)^{I+J+F} \times \begin{Bmatrix} I & J & F \\ J' & I & 1 \end{Bmatrix} \\ &\times \langle \gamma J || T^{(1)} || \gamma' J' \rangle \langle I || M^{(1)} || I \rangle. \end{aligned} \quad (2)$$

The reduced nuclear matrix element is not calculated, but the conventional definition of the nuclear magnetic dipole moment is used,

$$\langle I || M^{(1)} || I \rangle = \mu_I. \quad (3)$$

Using Wigner-Eckarts theorem, the reduced matrix element is given by

$$\langle I || M^{(1)} || I \rangle = \mu_I \sqrt{\frac{(2I+1)(I+1)}{I}} \quad (4)$$

and the hyperfine interaction can be calculated using

$$\begin{aligned} \langle \gamma J I F M_F | \mathbf{T}^{(1)} \cdot \mathbf{M}^{(1)} | \gamma' J' I F M_F \rangle &= (-1)^{J+J'+F} \\ &\times \mu_I \sqrt{\frac{(2I+1)(I+1)}{I}} \begin{Bmatrix} I & J & F \\ J' & I & 1 \end{Bmatrix} \langle \gamma J || T^{(1)} || \gamma' J' \rangle. \end{aligned} \quad (5)$$

In this work the nuclear magnetic dipole moments for the

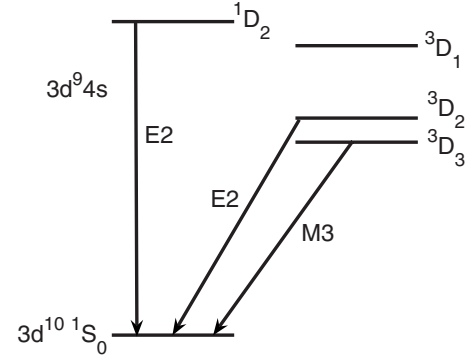


FIG. 1. An overview of the first excited levels in the Ni-like system and the transitions of interest in this work.

different isotopes were taken from Kurucz [24]. When calculating the hyperfine interaction for different isotopes of the same ion and for different hyperfine levels belonging to the same fine structure level, the differences in magnitude are given by μ_I and the analytic expression before the reduced matrix element. To be able to investigate the potential importance of the hyperfine interaction we therefore define the electronic hyperfine constant $A_{\text{hpf}}^{\text{elec}}$, which is independent of isotope and F value, as

$$A_{\text{hpf}}^{\text{elec}}(\gamma J, \gamma' J') = \langle \gamma J || T^{(1)} || \gamma' J' \rangle. \quad (6)$$

B. Hyperfine induced transitions

There are two different hyperfine mixing which could be important for the lifetime of the $3d^9 4s\ ^3D_3$ level, namely, mixing with the $3d^9 4s\ ^3D_2$ and $1D_2$ levels. By using first order perturbation theory, the mixing with these two levels are given by

$$\begin{aligned} c(^x D_2 F) &= \mu_I \sqrt{\frac{(2I+1)(I+1)}{I}} \\ &\times \begin{Bmatrix} I & 2 & F \\ 3 & I & 1 \end{Bmatrix} \frac{\langle ^x D_2 || T^{(1)} || ^3 D_3 \rangle}{E_{3D_3} - E_{x D_2}}, \end{aligned} \quad (7)$$

where x refers to the singlet or the triplet.

The transition rate of the electric quadrupole transition between two hyperfine states $|\gamma J I F\rangle$ and $|\gamma' J' I F'\rangle$ is given by

$$A_{E2}(\gamma J I F, \gamma' J' I F') = \frac{(2\pi)^5}{15\lambda^5} \frac{1}{2F'+1} |\langle \gamma J I F || E^{(2)} || \gamma' J' I F' \rangle|^2, \quad (8)$$

where the reduced matrix element can be expressed as

$$\begin{aligned} \langle \gamma J I F || E^{(2)} || \gamma' J' I F' \rangle &= \sqrt{(2F+1)(2F'+1)} \\ &\times (-1)^{J+I+F'+2} \begin{Bmatrix} J & I & F \\ F' & 2 & J' \end{Bmatrix} \\ &\times \langle \gamma J || E^{(2)} || \gamma' J' \rangle. \end{aligned} \quad (9)$$

Using this and summing over all lower hyperfine levels de-

rived from the same fine structure level, the total transition rate from an upper hyperfine level to all lower is given by

$$A_{E2}(\gamma J, \gamma' J' IF') = \frac{(2\pi)^5}{15\lambda^5} \frac{1}{2J'+1} |\langle \gamma J || E^{(2)} || \gamma' J' \rangle|^2, \quad (10)$$

where we have used the fact that the difference in wavelength between the different hyperfine transitions is negligible.

Using this and Eq. (7) we can express the hyperfine induced electric quadrupole transition rate between $3d^{10}1S_0$ and $3d^94s^3D_3$ as

$$\begin{aligned} A_{\text{hpf-E2}}(1S_0 - 3D_3 F) &= \frac{(2\pi)^5}{15\lambda^5} \frac{1}{7} \mu_i^2 \frac{(2I+1)(I+1)}{I} \\ &\times \left\{ \begin{matrix} I & 2 & F \\ 3 & I & 1 \end{matrix} \right\}^2 \left| \frac{\langle 3D_2 || T^{(1)} || 3D_3 \rangle}{E_{3D_3} - E_{3D_2}} \right|^2 \\ &\times \langle 1S_0 || E^{(2)} || 3D_2 \rangle + \frac{\langle 1D_2 || T^{(1)} || 3D_3 \rangle}{E_{3D_3} - E_{1D_2}} \\ &\times \langle 1S_0 || E^{(2)} || 1D_2 \rangle \Big|^2. \end{aligned} \quad (11)$$

As mentioned in the Introduction, well-known examples of hyperfine quenching arise from the lowest excited level of many two electron systems $nsnp^3P_0$. Brage *et al.* [1] showed that for such systems and for low ionization stages, it is important to include both the mixing with $nsnp^3P_1$ and $1P_1$. For highly ionized Ni-like systems the $3d^94s^3D_2$ and $1D_2$ are close to jj coupled and therefore the values of the transition matrix elements for the $1S_0 - 3D_2$ and $1S_0 - 1D_2$ transitions are about equal, i.e.,

$$\langle 1S_0 || E^{(2)} || 3D_2 \rangle \approx \langle 1S_0 || E^{(2)} || 1D_2 \rangle. \quad (12)$$

Considering the mixing of $3D_2$ and $1D_2$ with $3D_3$ their relative size are related as

$$\frac{\langle 3D_2 || T^{(1)} || 3D_3 \rangle}{E_{3D_3} - E_{3D_2}} \gg \frac{\langle 1D_2 || T^{(1)} || 3D_3 \rangle}{E_{3D_3} - E_{1D_2}}. \quad (13)$$

Because of this the mixing with $1D_2$ becomes less important the more jj -coupled the system is and for the highly ionized Ni-like systems only the mixing with $3D_2$ is of importance. Hence for the higher Z member of the Ni sequence the hyperfine induced electric quadrupole transition rate is given by

$$\begin{aligned} A_{\text{hpf-E2}}(1S_0 - 3D_3 F) &= \frac{(2\pi)^5}{15\lambda^5} \frac{1}{7} \mu_i^2 \frac{(2I+1)(I+1)}{I} \\ &\times \left\{ \begin{matrix} I & 2 & F \\ 3 & I & 1 \end{matrix} \right\}^2 \left| \frac{\langle 3D_2 || T^{(1)} || 3D_3 \rangle}{E_{3D_3} - E_{3D_2}} \right|^2 \\ &\times \langle 1S_0 || E^{(2)} || 3D_2 \rangle \Big|^2. \end{aligned} \quad (14)$$

An equivalent form of this expression can be written as

$$\begin{aligned} A_{\text{hpf-E2}}(1S_0 - 3D_3 F) &= \mu_i^2 \frac{(2I+1)(I+1)}{I} \\ &\times \left\{ \begin{matrix} I & 2 & F \\ 3 & I & 1 \end{matrix} \right\}^2 \left(\frac{\langle 3D_2 || T^{(1)} || 3D_3 \rangle}{E_{3D_3} - E_{3D_2}} \right)^2 \\ &\times \left(\frac{E_{3D_3} - E_{1S_0}}{E_{3D_2} - E_{1S_0}} \right)^5 A_{E2}(1S_0 - 3D_2), \end{aligned} \quad (15)$$

where in the last row the $A_{E2}(1S_0 - 3D_2)$ transition rate has been rescaled to the $1S_0 - 3D_3$ transition energy. For the higher end of the Ni-like isoelectronic sequence the rescaling does not change the rate significantly, since the energy difference between $3D_3$ and $3D_2$ is very small compared to their excitation energies. To investigate the possible importance of the hyperfine induced transition channel along the isoelectronic sequence we define a hyperfine induced transition rate, similar to the hyperfine constant $A_{\text{hpf}}^{\text{elec}}$, which is independent of μ_i , I , and F as

$$\begin{aligned} A_{\text{hpf-E2}}^{\text{elec}}(1S_0 - 3D_3) &= \left(\frac{\langle 3D_2 || T^{(1)} || 3D_3 \rangle}{E_{3D_3} - E_{3D_2}} \right)^2 \\ &\times \left(\frac{E_{3D_3} - E_{1S_0}}{E_{3D_2} - E_{1S_0}} \right)^5 A_{E2}(1S_0 - 3D_2). \end{aligned} \quad (16)$$

C. The MCDHF method

The calculations were performed using the GRASPVP package (Parpia *et al.* [25]) which is based on the multiconfiguration Dirac-Hartree-Fock (MCDHF) method (Grant *et al.* [26]). Starting from the Dirac-Coulomb interaction

$$H_{\text{DC}} = \sum_i [c\alpha_i \cdot \mathbf{p}_i + (\beta_i - 1)c^2 + V_i^N] + \sum_{i>j} \frac{1}{r_{ij}}, \quad (17)$$

where V_i^N is the monopole part of the electron-nucleus Coulomb interaction, the atomic state functions (ASFs) were obtained as a linear combination of configuration state functions (CSFs)

$$|\Gamma JM_J\rangle = \sum_i c_i |\gamma_i JM_J\rangle, \quad (18)$$

where J and M_J are the angular and magnetic quantum number and γ_i denotes the configuration and all coupling information to uniquely define the state. The CSFs were built from one-electron Dirac orbitals and in the relativistic self-consistent field procedure both the radial part of these orbitals and the expansion coefficients c_i were optimized to self-consistency (Fischer *et al.* [27]). The Breit interaction

$$B_{ij} = -\frac{1}{2r_{ij}} \left[\alpha_i \cdot \alpha_j + \frac{(\alpha_i \cdot \mathbf{r}_{ij})(\alpha_j \cdot \mathbf{r}_{ij})}{r_{ij}^2} \right] \quad (19)$$

was included in a subsequent configuration interaction (CI) calculation (McKenzie *et al.* [28]).

From the ASFs a number of atomic properties were calculated. The parameters for a transition between the states $|\Gamma JM_J\rangle$ and $|\Gamma' JM'_J\rangle$ can be expressed in terms of reduced matrix elements

$$\langle \Gamma J || O || \Gamma' J' \rangle = \sum_{ij} c_i c_j \langle \gamma_i J || O || \gamma_j J' \rangle, \quad (20)$$

where O is the corresponding transition operator in the Coulomb or Babushkin gauge [29]. In this paper the upper and lower states were described by a linear combination of CSFs described by independently optimized Dirac orbital sets. To calculate the transition matrix element between two ASFs, biorthogonal transformations of the ASFs were performed (Olsen *et al.* [30]). In the new representation the matrix element could be evaluated using standard Racah algebra. Using expression (5) the hyperfine interaction was calculated from the reduced matrix elements in a similar way as above using a modified version of HFS92 (Jönsson *et al.* [31], Fischer and Jönsson [32])

D. Method of calculation

Our calculations are based on the restricted active space (RAS) method (Roos *et al.* [33], Olsen *et al.* [34], Brage and Fischer [35]). For the high- Z end of the sequence, these calculations are based on a quite straightforward approach, while for the elements close to the neutral end, relaxation effects for the orbitals are important and introduce some complications. Let us start by outlining the method for high Z .

1. High- Z approach

Separate calculations were performed for the lower ($3d^{10}$) and upper ($3d^9 4s$) configurations. The importance of different types of correlations were investigated and in the final calculation, correlations between the valance orbitals ($3d$ and $4s$) and core-valance correlation with the $3s$ and $3p$ cores were included. The active set of orbitals were expanded as

$$\text{AS1} = \{3s, 3p, 3d, 4s, 4p, 4d, 4f\},$$

$$\text{AS2} = \text{AS1} + \{5s, 5p, 5d, 5f\},$$

$$\text{AS3} = \text{AS2} + \{6s, 6p, 6d, 6f\},$$

TABLE II. Level structure of the $3d^9 4s$ configuration in Mo^{14+}

	$E(\text{cm}^{-1})$			
	3D_3	3D_2	3D_1	1D_2
AS1	0	5018	27603	32346
AS2	0	5068	27648	32476
AS3	0	5063	27648	32471
AS4	0	5060	27648	32467
+Breit	0	5059	26638	31444
Ref. [36]	0	4950	26860	31500

TABLE I. Excitation energy of the $3d^9 4s \ ^3D_3$ level in Mo^{14+}

	$E(\text{cm}^{-1})$
AS1	1699935
AS2	1693450
AS3	1692936
AS4	1692921
+Breit	1692941
Ref. [36]	1694910

$$\text{AS4} = \text{AS3} + \{7s, 8s\}.$$

In the first step, which we label Dirac-Fock, only the reference configurations were included and all orbitals of $3d^{10}$ and $3d^9 4s$ were optimized in independent extended average level calculations (EALs) [26]. In the second calculation we included single and double excitations from $3d$ and $4s$ and single excitations from $3s$ and $3p$ to the active set of orbitals AS1. Only the new orbitals were optimized and the others were kept fixed, i.e., all $n=4$ orbitals were optimized in the $3d^{10}$ calculation and $4p, 4d, 4f$ in the $3d^9 4s$ calculation. In the next step the calculations were enlarged allowing for the same types of excitations using AS2 and the $n=5$ orbitals were optimized. In the fourth step all CSF:s from last step were used and all single and double excitations to AS3 was added and the $n=6$ orbitals were optimized. By this step the calculations had converged, but to allow for spin-polarization (Jönsson [37], Lindgren and Morrison [38]) a fifth calculation was performed including all configurations from the last step and adding all single and double excitations, where one of the excitations was from $1s, 2s, 3s,$ or $4s$ and the other from $3d$ or $4s$ to AS4. All this resulted in an expansion of 79363 CSFs for the $3d^9 4s$ calculation. As the final step we added the transverse photon contributions, vacuum polarization and normal and specific mass shift to the Dirac-Coulomb Hamiltonian through a configuration interaction calculation. The convergence study of the results are given in Tables I–III.

2. Low- Z approach, with relaxation

Dong and Fritzsche [39] pointed out that relaxation effects are important in the low- Z end of the nickel-like se-

TABLE III. Convergence of the transition rate for the two $E2$ transitions $3d^{10} 1S_0-3d^9 4s 1,3D_2$ and the $M3$ transition $3d^{10} 1S_0-3d^9 4s 3D_3$ in Mo^{14+} .

	$A(\text{s}^{-1})$		
	$E2(1S_0-3D_2)$	$E2(1S_0-1D_2)$	$M3(1S_0-3D_3)$
AS1	8.33 [6]	1.18 [7]	3.21[-1]
AS2	8.26 [6]	1.17 [7]	3.26[-1]
AS3	8.32 [6]	1.18 [7]	3.31[-1]
AS4	8.32 [6]	1.18 [7]	3.31[-1]
+Breit	8.17 [6]	1.19 [7]	3.31[-1]

quence. This implies that the difference in the $3d$ orbitals between the ground $3d^{10}$ and excited $3d^9 4s$ are significant and this needs to be handled carefully. To take this into account we use a simplistic, but quite effective, method for Cu^+ .

The first step is a Dirac-Hartree-Fock EAL calculation for the excited $3d^9 4s$. To model the ground level, we then use the same orbitals and optimize a $4d$ on the expansion

$$\{3d^{10} + 3d^9 4d\} 1S_0.$$

This was also used as a multi-reference set in the calculations for the ground level. It is after this first step possible to perform the calculation for the two configurations independently, while keeping the orbitals up to $3d$ fixed.

The calculations were then expanded in the same manner as for the high- Z approach. The convergence study of the excitation energy of the $3d^9 4s 3D_3$ level and the energy splitting of the $3d^9 4s$ configuration is given in Table IV and V.

III. RESULTS AND DISCUSSION

In Tables I–III a convergence study of the calculations for Mo^{14+} is presented. From Tables I and II it is found that the excitation energies and the energy splittings between the levels of the $3d^9 4s$ configuration converged as the calculations were systematically enlarged. Hence the CI calculations was of limited importance for both the excitation energies and the fine structure splitting of $3d^9 4s 3D$, whereas it changed the term splitting between $3D$ and $1D$ by 3%. It is also found that the current calculations are in excellent agreement with experimental energies. From Table III it can also be seen that the transition rates converged quickly and that the inclusion

TABLE IV. Excitation energy of the $3d^9 4s 3D_3$ level in Cu^+ .

	$E(\text{cm}^{-1})$
DF	38104
AS1	24305
AS2	22933
AS3	22541
AS4	22392
+Breit	22469
Ref. [36]	21928.754

of further relativistic effects was of limited importance and had a maximal importance for the $3d^{10} 1S_0-3d^9 4s 3D_2$ $E2$ transition rate, which was lowered by 1.8%.

The calculations for Cu^+ was based on a slightly different model. In Tables IV and V our excitation energies and level splittings are presented and it is found that our calculations are in excellent agreement with experimental values. Table VI indicates that the hyperfine induced transition dominates the decay of the $3D_3$. The resulting lifetime is very long, so this case can be seen as more of theoretical interest.

In the theory section we discussed the importance of including the mixing with $3d^9 4s 1D_2$. A study of this importance is presented in Table VI where the magnetic octupole transition rate A_{M3} the hyperfine induced transition rate $A_{\text{hpf-}E2}$, both with the mixing with $1D_2$ included and omitted, and the total transition rate A_{tot} are presented for Cu^+ , Mo^{14+} , and Xe^{26+} . From this it is obvious that it is important to include the mixing with $1D_2$ in the beginning of the isoelectronic sequence whereas $A_{\text{hpf-}E2}$ is completely dominated by the $3D_2$ mixing when dealing with heavily ionized Ni-like ions. Including the $1D_2$ mixing change A_{tot} with about 120% for Cu^+ , 5% for Mo^{14+} , and only 1% for Xe^{26+} . As will be seen in the discussion of Table VII 5% could be considered within the error bars, and for simplicity we will present all other results excluding the $1D_2$ mixing. To claim higher precision of the calculations, the nuclear electric quadrupole hyperfine interaction should also be included.

The results are presented in detail in Table VII and an overview of the results along the isoelectronic sequence, except Cu^+ , is presented in Figs. 1–3. In Fig. 2 we have plotted the hyperfine induced transition rate $A_{\text{hpf-}E2}$ relative to the

TABLE V. Level structure of the $3d^9 4s$ configuration in Cu^+ .

	$E(\text{cm}^{-1})$			
	$3D_3$	$3D_2$	$3D_1$	$1D_2$
DF	0	1003	2152	5033
AS1	0	981	2155	4756
AS2	0	965	2170	4554
AS3	0	959	2173	4499
AS4	0	957	2174	4476
+Breit	0	912	2026	4371
Ref. [36]	0	918.377	2069.627	4335.814

TABLE VI. Rates in s^{-1} from different approaches (see text) for the $3d^{10} 1S_0 - 3d^9 4s 3D_3$ transition. ($a[b]=a \times 10^b$) μ from Ref. [24].

F	A_{M3}	only $3D_2$		include $1D_2$	
		$A_{\text{hpf-}E2}$	A_{tot}	$A_{\text{hpf-}E2}$	A_{tot}
$^{63}\text{Cu } I=3/2 \mu=2.2233$					
9/2	3.097[-12]	0.0	3.10[-12]	0.0	3.10[-12]
7/2	3.097[-12]	4.127[-9]	4.13[-9]	9.191[-9]	9.19[-9]
5/2	3.097[-12]	3.913[-9]	3.92[-9]	8.715[-9]	8.72[-9]
3/2	3.097[-12]	1.926[-9]	1.93[-9]	4.289[-9]	4.29[-9]
$^{65}\text{Cu } I=3/2 \mu=2.3817$					
9/2	3.097[-12]	0.0	3.10[-12]	0.0	3.19[-12]
7/2	3.097[-12]	4.736[-9]	4.74[-9]	1.055[-8]	1.06[-8]
5/2	3.097[-12]	4.490[-9]	4.49[-9]	1.000[-8]	1.00[-8]
3/2	3.097[-12]	2.210[-9]	2.21[-9]	4.922[-9]	4.93[-9]
$^{95}\text{Mo } I=5/2 \mu=-0.9142$					
11/2	3.31[-1]	0.0	3.31[-1]	0.0	3.31[-1]
9/2	3.31[-1]	8.47[-1]	1.178	9.05[-1]	1.236
7/2	3.31[-1]	9.85[-1]	1.316	1.053	1.384
5/2	3.31[-1]	7.48[-1]	1.079	7.80[-1]	1.121
3/2	3.31[-1]	3.94[-1]	7.25[-1]	4.21[-1]	7.53[-1]
1/2	3.31[-1]	1.08[-1]	4.39[-1]	1.15[-1]	4.46[-1]
$^{129}\text{Xe } I=1/2 \mu=-0.7780$					
7/2	6.62 [1]	0.0	6.62 [1]	0.0	6.62 [2]
5/2	6.62 [1]	2.861 [2]	3.522 [2]	2.899 [2]	3.560 [2]

magnetic octupole transition rate, A_{M3} . For ions with two different isotopes with a nonzero nuclear spin, the relative transition rates for both are shown in the diagram. Depending on the nuclear spin I of an isotope, there are always one or two hyperfine levels which cannot mix with $3D_2$ (or $1D_2$) and these have been excluded from the plot since they do not have an electric quadrupole decay channel. From this figure it is clear that the hyperfine induced transition is important for all isotopes studied in this work and for some of them this is the dominating decay channel. From Table VII it is seen that even for Pd where $A_{\text{hpf-}E2}$ is least important, $A_{\text{hpf-}E2}$ is stronger than A_{M3} for some hyperfine levels.

The hyperfine induced transition varies with the nuclear magnetic dipole moment μ_I according to

$$A_{\text{hpf-}E2} \propto \mu_I^2. \quad (21)$$

Since the isotopes have different μ_I it is hard to draw any conclusion about the isoelectronic sequence using the normal relative intensities. $A_{\text{hpf-}E2}$ also has an F dependence, and since the isotopes have different nuclear spin, we have plotted $A_{\text{hpf-}E2}^{\text{elec}}$, defined in Eq. (16), relative to A_{M3} in Fig. 2 along the sequence (the dashed line) to be able to draw conclusions about the importance of the hyperfine induced decay channel along the isoelectronic sequence. The trend in the diagram shows that the hyperfine induced transition channel can be expected to be most important in the lower end of the sequence and the importance appears to level out going to the higher end. Also taking the result for Cu^+ , $A_{\text{hpf-}E2}^{\text{elec}}/A_{M3} \approx 3$, into consideration we conclude that the hyperfine induced transition is important for all Ni-like isotopes with a nuclear

spin unless the nuclear magnetic dipole moment is extremely small.

In Fig. 3 the different isotope and F -dependent lifetimes for each ion are plotted on a logarithmic scale and it is obvious that the hyperfine induced transition can have an enormous impact on the lifetime. The longest lifetime for each ion are those states which do not have any hyperfine mixing and are determined by the magnetic octupole transition rate. The Z dependence of magnetic octupole transitions should be

$$A_{M3} \propto (Z - \sigma)^{10}, \quad (22)$$

where σ is the screening parameter. To test our calculations, a function of the form $k(Z - \sigma)^{-10}$ has been fitted to the longest lifetimes and we found that we could get a good fit using $\sigma=24.5$.

In Tables VIII and IX comparisons with other results are presented. Before the publication of our recent paper (Yao *et al.* [17,18]), no calculations known to us included the hyperfine induced branches and have only treated the decay of the $3D_3$ as pure $M3$.

In Table VIII we have compared both the $3d^{10} 1S_0 - 3d^9 4s 3D_3$ $M3$ transition rate and the two $E2$ transition rates $3d^{10} 1S_0 - 3d^9 4s 3D_2$ and $3d^{10} 1S_0 - 3d^9 4s 3D_2$ with other works. The latter two are important, since they are the driving transitions behind the hyperfine induced channel. In relativistic quantum mechanics the $E2$ transition rates can be calculated using either the Babushkin or the Coulomb gauge, which are equivalent to the length and the velocity form in the nonrelativistic quantum mechanics. The Babushkin gauge is the most reliable of the two, but both gauges should

TABLE VII. Transition rates and lifetimes of the $3d^9 4s \ ^3D_3$ hyperfine levels along the Ni-like isoelectronic sequence. A_{M3} is the magnetic octupole transition rate, $A_{\text{hpf-E2}}$ the F -dependent hyperfine induced electric quadrupole transition rate, A_{tot} the F -dependent total transition rate and τ the F -dependent lifetime. All transition rates are given in s^{-1} . μ from Ref. [24].

F_i	A_{M3}	$A_{\text{hpf-E2}}$	A_{tot}	τ (ms)
^{95}Mo $I=5/2$ $\mu=-0.9142$				
11/2	0.331	0.0	0.331	3.02×10^3
9/2	0.331	0.847	1.18	849
7/2	0.331	0.985	1.32	760
5/2	0.331	0.748	1.08	927
3/2	0.331	0.394	0.725	1.38×10^3
1/2	0.331	0.108	0.439	2.28×10^3
^{97}Mo $I=5/2$ $\mu=-0.9335$				
11/2	0.331	0.0	0.331	3.02×10^3
9/2	0.331	0.875	1.21	829
7/2	0.331	1.02	1.35	741
5/2	0.331	0.773	1.10	906
3/2	0.331	0.407	0.738	1.36×10^3
1/2	0.331	0.111	0.442	2.26×10^3
^{105}Pd $I=5/2$ $\mu=-0.642$				
11/2	2.82	0.0	2.82	355
9/2	2.82	3.01	5.83	172
7/2	2.82	3.50	6.33	158
5/2	2.82	2.66	5.48	182
3/2	2.82	1.41	4.22	237
1/2	2.82	0.383	3.20	313
^{113}In $I=9/2$ $\mu=5.5289$				
15/2	10.6	0.0	10.6	92.6
13/2	10.6	586	596	1.68
11/2	10.6	777	788	1.27
9/2	10.6	711	721	1.39
7/2	10.6	500	510	1.96
5/2	10.6	239	249	4.01
3/2	10.6	0.0	10.6	92.6
^{115}In $I=9/2$ $\mu=5.5408$				
15/2	10.6	0.0	10.6	92.6
13/2	10.6	588	599	1.67
11/2	10.6	781	791	1.26
9/2	10.6	714	724	1.38
7/2	10.6	502	513	1.95
5/2	10.6	240	250	4.00
3/2	10.6	0.0	10.6	92.6
^{121}Sb $I=5/2$ $\mu=3.3634$				
11/2	23.0	0.0	23.0	43.5
9/2	23.0	604	627	1.59
7/2	23.0	703	726	1.38
5/2	23.0	534	557	1.80
3/2	23.0	281	304	3.29
1/2	23.0	76.9	99.9	10.0
^{123}Sb $I=7/2$ $\mu=2.5498$				
13/2	23.0	0.0	23.0	43.5
11/2	23.0	293	316	3.16

TABLE VII. (Continued.)

F_i	A_{M3}	$A_{\text{hpf-E2}}$	A_{tot}	τ (ms)
9/2	23.0	371	394	2.54
7/2	23.0	319	342	2.92
5/2	23.0	206	229	4.36
3/2	23.0	87.0	110	9.09
1/2	23.0	0.0	23.0	43.5
^{127}I I=5/2 $\mu=2.8133$				
11/2	47.2	0.0	47.2	21.2
9/2	47.2	848	895	1.12
7/2	47.2	987	1.03×10^3	0.967
5/2	47.2	749	797	1.26
3/2	47.2	395	442	2.26
1/2	47.2	108	155	6.45
^{129}Xe I=1/2 $\mu=-0.7780$				
7/2	66.2	0.0	66.2	15.1
5/2	66.2	286	352	2.84
^{131}Xe I=3/2 $\mu=0.6919$				
9/2	66.2	0.0	66.2	15.1
7/2	66.2	96.4	163	6.15
5/2	66.2	92.5	157	6.30
3/2	66.2	46.0	112	8.92
^{133}Cs I=7/2 $\mu=2.5820$				
13/2	91.6	0.0	91.6	10.9
11/2	91.6	1.15×10^3	1.25×10^3	0.803
9/2	91.6	1.46×10^3	1.55×10^3	0.644
7/2	91.6	1.26×10^3	1.35×10^3	0.742
5/2	91.6	812	903	1.11
3/2	91.6	343	424	2.36
1/2	91.6	0.0	91.6	10.9
^{135}Ba I=3/2 $\mu=0.8379$				
9/2	125	0.0	125	8.00
7/2	125	268	393	2.54
5/2	125	254	379	2.64
3/2	125	125	250	4.00
^{137}Ba I=3/2 $\mu=0.9374$				
9/2	125	0.0	125	8.00
7/2	125	336	461	2.17
5/2	125	318	443	2.26
3/2	125	157	282	3.55
^{141}Pr I=5/2 $\mu=4.136$				
11/2	302	0.0	302	3.31
9/2	302	1.16×10^4	1.19×10^4	0.0841
7/2	302	1.35×10^4	1.38×10^4	0.0725
5/2	302	1.02×10^4	1.05×10^4	0.0949
3/2	302	5.39×10^3	5.70×10^3	0.176
1/2	302	1.48×10^3	1.78×10^3	0.563
^{143}Nd I=7/2 $\mu=1.065$				
13/2	397	0.0	397	2.52
11/2	397	859	1.26×10^3	0.796

TABLE VII. (Continued.)

F_i	A_{M3}	$A_{\text{hpf-E2}}$	A_{tot}	τ (ms)
9/2	397	1.09×10^3	1.48×10^3	0.674
7/2	397	935	1.33×10^3	0.751
5/2	397	604	1.00×10^3	0.999
3/2	397	255	652	1.53
1/2	397	0.0	397	2.52
$^{145}\text{Nd } I=7/2 \mu=0.656$				
13/2	397	0.0	397	2.52
11/2	397	326	723	1.38
9/2	397	413	810	1.24
7/2	397	355	752	1.33
5/2	397	229	626	1.60
3/2	397	96.7	494	2.03
1/2	397	0.0	397	2.52

give the same result, so a comparison of the two give a good indication of the accuracy. In Table VIII we have presented the transition rates in both gauges and we find good agreement between the two for all ions except Cu^+ . The accuracy of the Cu^+ calculation could therefore be expected to be lower than for the other ions.

Träbert *et al.* [15] performed calculations of the $M3$ and the two $E2$ transition rates using the multiconfiguration Dirac-Hartree-Fock method for Xe^{26+} and from Table VIII it is seen that their $E2$ transition rates are in good agreement with ours, whereas their $M3$ transition rate is 8% higher than ours. Biémont [14] did calculations for the three transition rates of interest, also using the multiconfiguration Dirac-Hartree-Fock method, for Nd^{32+} . From Table VIII it is found that all their rates are higher than ours by 5–9%. It is hard to draw any conclusions from comparing our calculation with those presented in [14,15] since both of those works are limited to just one ion.

Safronova *et al.* [16] performed theoretical calculations, using the relativistic many-body perturbation theory

(RMBPT), for all ions included in this work except Cu^+ . Comparing the $M3$ transition rates along the isoelectronic sequence it is found that all their results are lower than ours, ranging from 33% lower for Mo^{14+} in the beginning of the sequence, to 15% for Nd^{32+} toward the end of the sequence. Comparing the $E2$ transition rates for the $3d^{10}1S_0 - 3d^94s^3D_2$ transition the same pattern is found. Again their rates are lower than ours, (35% for Mo^{14+} down to 13% for Nd^{32+}). Making the same comparison for the $3d^{10}1S_0 - 3d^94s^1D_2$ $E2$ transition rates again the same pattern is found with their rate being 29% lower for Mo^{14+} going down to 12% for Nd^{32+} . From these comparisons it seems likely that there are some systematic differences between our two theoretical models or methods. Safronova *et al.* [16] include the same type of correlations as used in our work, i.e., valance correlation and core-valance correlation with $3s$ and $3p$, but made large spectroscopic calculations of the Ni-like system including 76 different transitions whereas we have concentrated on a few transitions. Comparing the transition en-

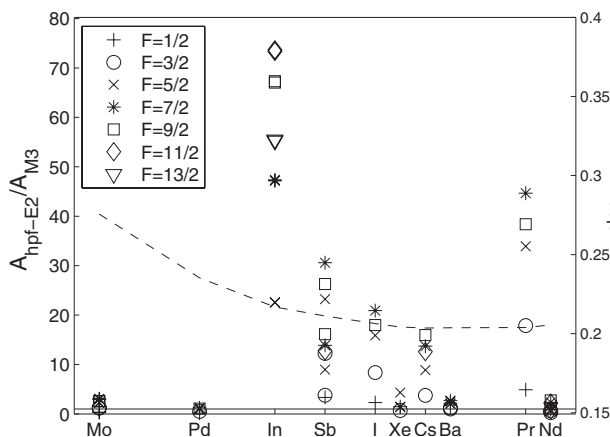


FIG. 2. The hyperfine induced $E2$ transition rate relative the $M3$ transition rate for the $3d^{10}1S_0 - 3d^94s^3D_3$ transition along the Ni-like isoelectronic sequence, together with the smoothly varying A^{elec}/A^{M3} (dashed curve).

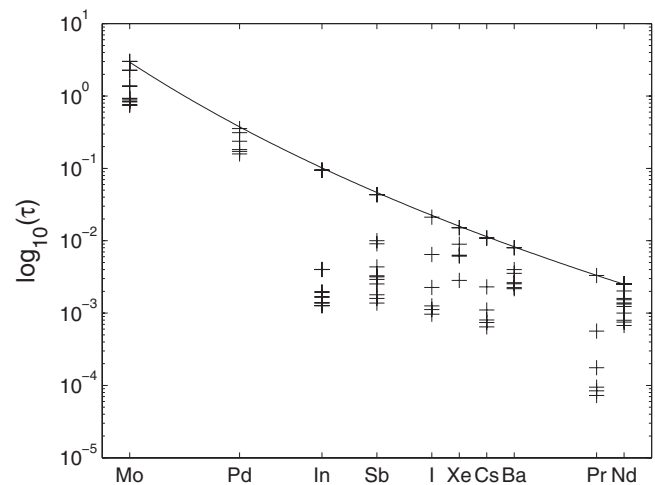


FIG. 3. The F -dependent lifetimes (+) of the $3d^94s^93D_3$ hyperfine levels along the Ni-like isoelectronic sequence. The solid line depicts the theoretical lifetimes associated to pure $M3$ transitions.

TABLE VIII. Comparisons of our transition rates with earlier results. All others works treated the $3d^{10} {}^1S_0-3d^9 4s {}^3D_3$ transition as a pure $M3$ transition. All transition rates are given in s^{-1} .

ion	${}^1S_0-{}^3D_3(M3)$		${}^1S_0-{}^3D_2(E2)$			${}^1S_0-{}^1D_2(E2)$		
	Our	Other	Our	Other		Our	Other	
			Babushkin	Coulomb	Babushkin	Coulomb		
Cu ⁺	3.10×10^{-12}		0.104	0.157		1.937	2.687	
Mo ¹⁴⁺	0.331	0.223 ^a	8.17×10^6	8.10×10^6	5.29×10^6 ^a	1.19×10^7	1.18×10^7	8.43×10^6 ^a
Pd ¹⁸⁺	2.82	2.03 ^a	3.46×10^7	3.43×10^7	2.67×10^7 ^a	4.01×10^7	3.98×10^7	3.15×10^7 ^a
In ²⁰⁺	10.6	7.90 ^a	8.21×10^7	8.14×10^7	6.69×10^7 ^a	8.49×10^7	8.42×10^7	6.97×10^7 ^a
Sb ²³⁺	23.0	17.7 ^a	1.36×10^8	1.35×10^8	1.12×10^8 ^a	1.33×10^8	1.32×10^8	1.10×10^8 ^a
I ²⁵⁺	47.2	37.8 ^a	2.15×10^8	2.14×10^8	1.81×10^8 ^a	2.00×10^8	1.99×10^8	1.68×10^8 ^a
Xe ²⁶⁺	66.2	53.1 ^a	2.67×10^8	2.65×10^8	2.26×10^8 ^a	2.43×10^8	2.41×10^8	2.06×10^8 ^a
		66.4 ^b						
		71.4 ^c			2.72×10^8 ^c			2.49×10^8 ^c
Cs ²⁷⁺	91.6	75.5 ^a	3.29×10^8	3.26×10^8	2.81×10^8 ^a	2.93×10^8	2.91×10^8	2.48×10^8 ^a
Ba ²⁸⁺	125	104 ^a	4.01×10^8	3.98×10^8	3.44×10^8 ^a	3.52×10^8	3.50×10^8	2.96×10^8 ^a
Pr ³¹⁺	302	255 ^a	6.98×10^8	6.92×10^8	6.07×10^8 ^a	5.87×10^8	5.83×10^8	5.15×10^8 ^a
Nd ³²⁺	397	337 ^a	8.30×10^8	8.23×10^8	7.24×10^8 ^a	6.89×10^8	6.84×10^8	6.06×10^8 ^a
		418 ^a			8.86×10^8 ^d			7.50×10^8 ^d

^aTheoretical, many body perturbation theory [16].

^bExperimental [19].

^cTheoretical, multiconfiguration Dirac-Hartree-Fock method [15].

^dTheoretical, multiconfiguration Dirac-Hartree-Fock method [14].

ergies from our and their calculations it is found that we are in good agreement, and even if the $M3$ transition scales with the energy to the power of seven, rescaling the transition rates only brings our results about 1% closer to each other at maximum. Correlation effects are in general most important for ions of low ionization stages and decrease with increasing Z . Considering that Safronova *et al.* results approach ours for high Z , it seems likely that Safronova *et al.* did not caught all important correlation for the $3d^9 4s$ levels in their large scale spectroscopic calculation of the Ni-like system.

The last comparison is with a recent paper by Träbert *et al.* [19] that followed our paper [17,18], where we explained the differences between theory and experiment in the previous experimental work by Träbert *et al.* [15]. In Ref. [19] Träbert *et al.* made lifetime measurements of the $3d^9 4s {}^3D_3$ level in ${}^{132}\text{Xe}$, an isotope without nuclear spin, and ${}^{129}\text{Xe}$, an isotope with a nuclear spin of $I=1/2$. The 3D_3 level in ${}^{132}\text{Xe}$ can only decay through the $M3$ transition channel and from

Table IX it is found that their results are in excellent agreement with our calculations. This is also true for their experimental lifetimes of the two hyperfine levels $F=7/2$ and $F=5/2$ in ${}^{129}\text{Xe}$, where the former is a pure $M3$ transition whereas the latter has a hyperfine induced $E2$ transition channel. These results give us confidence in our results also for the other ions in the isoelectronic sequence.

IV. CONCLUSIONS

An investigation of the lifetime of the $3d^9 4s {}^3D_3$ level along a part of the Ni-like isoelectronic sequence has been presented. The importance of the hyperfine induced electric quadrupole transition channel for isotopes with a nonzero nuclear magnetic dipole moment has been evaluated and it has been found that the lifetime of the $3d^9 4s {}^3D_3$ level is sensitive to this transition channel for all Ni-like ions in the range $Z=29$ to 60. We have found excellent agreement be-

TABLE IX. Comparison of our calculated lifetime of the $3d^9 4s {}^3D_3$ level with measurements by Träbert *et al.* [19]

isotope	I	F	Our	Lifetime (ms)		
				[19] ^a	[16] ^b	[15] ^c
${}^{132}\text{Xe}$	0		15.1	15.06 ± 0.24	18.6	14.0
${}^{129}\text{Xe}$	1/2	7/2	15.1	15.1 ± 0.5		
	1/2	5/2	2.84	2.7 ± 0.1		

^aExperimental.

^bRelativistic many-body perturbation calculation.

^cMulticonfiguration Hartree-Fock calculation, GRASPVC code.

tween our theoretical results and Träbert *et al.* [19] measurements of the lifetime of the level in ^{129}Xe and ^{132}Xe which give us confidence in our results not only for Xe^{26+} , but also for the other ions.

Further investigation of this system would be of interest. To further investigate the accuracy of our theoretical results for the isoelectronic sequence we can suggest a few measurements similar to those by Träbert *et al.* in Ref. [19], but for other ions. Isotopes with spin $I=1/2$ are preferable from an experimental point of view, since then there will only be two hyperfine levels, one with a pure $M3$ transition channel and one with the additional hpf- $E2$ channel. Unfortunately there are only a few of these isotopes. A more limited measurement, where only the lifetime of the states without hyperfine mixing would also be of interest. A good candidate for such a test of the $M3$ transition rate would be Ce^{30+} which has no natural isotopes with nuclear spin. Another possibility is to look for ions with large magnetic nuclear moments. A candidate for this would be indium. This ion has two isotopes, 5% ^{113}In and 95% ^{115}In , both with nuclear spin $I=9/2$ and very similar nuclear magnetic dipole moment $\mu_I(113)=5.53$ and $\mu_I(115)=5.54$, resulting in $\tau=92.6$ ms for F

$=15/2, 3/2$ and τ ranging from 1.26 to 4.01 ms for the other hyperfine levels. Because of the large differences in lifetime between the states with and without hyperfine mixing it might be possible to measure the lifetime of the $F=15/2, 3/2$ hyperfine levels rather accurately. Since the hyperfine induced $E2$ transition rates are sensitive to the $3d^{10}1S_0-3d^94s^3D_2$ $E2$ transition rate, comparisons with experimental lifetime measurements of the $3d^94s^3D_2$ level would be of great interest, but to our knowledge no such results are available.

ACKNOWLEDGMENTS

This work was supported by the National Natural Science Foundation of China under Grants No. 10704019 and No. 10574029, and China Postdoctoral Science Foundation. This work was also partly supported by a grant from the Swedish Research Council (Vetenskapsrådet) and Kungliga Fysiografiska Sällskapet i Lund. It is also partially supported by Shanghai Leading Academic Discipline Project, Project No. B107.

-
- [1] T. Brage, P. G. Judge, A. Aboussaïd, M. R. Godefroid, P. Jönsson, A. Ynnerman, C. F. Fischer, and D. S. Leckrone, *Astrophys. J.* **500**, 507 (1998).
- [2] 2006Y. Liu, R. Hutton, Y. Zou, M. Andersson, and T. Brage, *J. Phys. B* **39**, 3147 (2006).
- [3] C. Z. Dong, S. Fritzsche, G. Gaigalas, T. Jacob, and J. E. Sienkeiwicz, *Phys. Scr.* **T92**, 314 (2001).
- [4] U. I. Safronova, W. R. Johnson, and J. R. Albritton, *Phys. Rev. A* **62**, 052505 (2000).
- [5] C. L. Cocke, S. L. Varghese, J. A. Bednar, C. P. Bhalla, B. Curnutte, R. Kauffman, P. Randall, P. Richard, C. Woods, and J. H. Scofield, *Phys. Rev. A* **12**, 2413 (1975).
- [6] M. Klapisch, J. L. Schwob, M. Finkenthal, B. S. Fraenkel, S. Egert, A. Bar-Shalom, C. Breton, C. DeMichelis, and M. Mattioli, *Phys. Rev. Lett.* **41**, 403 (1978).
- [7] J. F. Wyart, C. Bauche-Arnoult, J. C. Gauthier, J. P. Geindre, P. Monier, M. Klapisch, A. Bar-Shalom, and A. Cohn, *Phys. Rev. A* **34**, 701 (1986).
- [8] P. Mandelbaum, J. F. Seely, U. Feldman, C. M. Brown, D. R. Kania, W. H. Goldstein, R. L. Kauffman, S. Langer, and A. Bar-Shalom, *Phys. Rev. A* **45**, 7480 (1992).
- [9] R. Doron, M. Fraenkel, P. Mandelbaum, A. Zigler, and J. L. Schwob, *Phys. Scr.* **58**, 19 (1998).
- [10] I. Y. Skobelev *et al.*, *J. Phys. B* **32**, 113 (1999).
- [11] A. Rahman, E. C. Hammarsten, S. Sakadzic, J. J. Rocca, and J. F. Wyart, *Phys. Scr.* **67**, 414 (2003).
- [12] A. Rahman, J. J. Rocca, and J. F. Wyart, *Phys. Scr.* **70**, 21 (2004).
- [13] P. Beiersdorfer, A. L. Osterheld, J. Scofield, B. Wargelin, and R. E. Marrs, *Phys. Rev. Lett.* **67**, 2272 (1991).
- [14] E. Biémont, *J. Phys. B* **30**, 4207 (1997).
- [15] E. Träbert, P. Beiersdorfer, G. V. Brown, K. Boyce, R. L. Kelley, C. A. Kilbourne, F. S. Porter, and A. Szymkowiak, *Phys. Rev. A* **73**, 022508 (2006).
- [16] U. I. Safronova, A. S. Safronova, S. M. Hamasha, and P. Beiersdorfer, *At. Data Nucl. Data Tables* **92**, 47 (2006).
- [17] K. Yao, M. Andersson, T. Brage, R. Hutton, P. Jönsson, and Y. Zou, *Phys. Rev. Lett.* **97**, 183001 (2006).
- [18] K. Yao, M. Andersson, T. Brage, R. Hutton, P. Jönsson, and Y. Zou, *Phys. Rev. Lett.* **98**, 269903(E) (2007).
- [19] E. Träbert, P. Beiersdorfer, and G. V. Brown, *Phys. Rev. Lett.* **98**, 263001 (2007).
- [20] L. D. Huff and W. V. Houston, *Phys. Rev.* **36**, 842 (1930).
- [21] H. Bergström, C. Levinson, H. Lundberg, S. Svanberg, C. G. Wahlström, and Zhao You Yuan, *Phys. Rev. A* **33**, 2387 (1986).
- [22] S. Mannervik, L. Broström, J. Lidberg, L.-O. Norlin, and P. Royen, *Phys. Rev. Lett.* **76**, 3675 (1996).
- [23] I. Lindgren and A. Rosén, *Case Stud. At. Phys.* **4**, 97 (1974).
- [24] R. L. Kurucz, *Phys. Scr.* **T47**, 110 (1993).
- [25] F.-A. Parpia, C. F. Fischer, and I. P. Grant, *Comput. Phys. Commun.* **94**, 249 (1996).
- [26] I. P. Grant, B. J. McKenzie, P. H. Norrington, D. F. Mayers, and N. C. Pyper, *Comput. Phys. Commun.* **21**, 207 (1980).
- [27] C. F. Fischer, T. Brage, and P. Jönsson, *Computational Atomic Structure. An MCHF Approach* (Institute of Physics Publishing, Bristol, Philadelphia, 1997).
- [28] B. J. McKenzie, I. P. Grant, and P. H. Norrington, *Comput. Phys. Commun.* **21**, 233 (1980).
- [29] I. P. Grant, *J. Phys. B* **7**, 1458 (1974).
- [30] J. Olsen, M. R. Godefroid, P. Jönsson, P. A. Malmqvist, and C. F. Fischer, *Phys. Rev. E* **52**, 4499 (1995).
- [31] P. Jönsson, F. A. Parpia, and C. F. Fischer, *Comput. Phys. Commun.* **96**, 301 (1996).
- [32] C. F. Fischer and P. Jönsson, *J. Mol. Struct.* **537**, 55 (2001).
- [33] B. O. Roos, P. R. Taylor, and P. E. M. Siegbahn, *Chem. Phys.*

- 48**, 157 (1980).
- [34] J. Olsen, B. O. Roos, P. Jørgensen, and H. Jensen, *J. Chem. Phys.* **89**, 2185 (1988).
- [35] T. Brage and C. F. Fischer, *Phys. Scr.* **T47**, 18 (1993).
- [36] Y. Ralchenko, F. Jou, D. Kelleher, A. Kramida, A. Musgrove, J. Reader, W. Wiese, and K. Olsen, National Institute of Standard and Technology, Gaithersburg, MD, NIST Atomic Spectra Database (version 3.1.2) (online), <http://physics.nist.gov/asd3>
- [37] P. Jönsson, *Phys. Scr.* **48**, 678 (1993).
- [38] I. Lindgren and J. Morrison, *Atomic Many-Body Theory*, Vol. 13, *Springer Series in Chemical Physics* (Springer-Verlag, Berlin, 1982).
- [39] C. Z. Dong and S. Fritzsche, *Phys. Rev. A* **72**, 012507 (2005).